# ABSTRACTS OF PAPERS DEPOSITED AT VINITI *

## HEAT AND MASS TRANSFER DURING DRYING OF A GRANULAR MATERIAL MOVING ALONG A HOT CHANNEL

V. V. Kornaraki

UDC 536.24.001:66.047.75

Heat and mass transport during drying of a compacted layer is considered, with the layer moving in a slot or a cylindrical channel with walls permeable to heat and water. The following assumptions are made: 1) the motion of the bed is stable and is of rod type; 2) the structure and porosity are unvarying; 3) the transport characteristics are constant; 4) the distributions of temperature and water content in the input section are uniform; 5) the heat transport due to concentration-dependent diffusion is negligible, as is that due to thermal diffusion; and 6) the longitudinal molecular transport of heat and matter is negligible by comparison with the convective transfer. The power is considered as a quasihomogeneous medium having effective transport coefficients. The temperature differences between the components are negligible.

A boundary-layer technique is employed on the basis that effective thermal and diffusion boundary layers are set up; two stages are distinguished: in the first, the thicknesses of the layers increase, while in the second the thicknesses attain half the width of the channel. The distributions for the temperature and potentials are taken as polynomials $T = A_0 + A_1Y + A_2Y^2$; $\theta = B_0 + B_1Y + B_2Y^2$; relationships are derived for the temperature, potentials, boundary-layer thicknesses, and stabilization lengths. A local heat-transfer coefficient is used in evaluating the heat-transfer rate, which is referred to the temperature difference between the wall and the flow in a given section; then the following equations are derived for a slot channel:

$$\text{Stage I} \qquad (X < X_q^{ss})\ \mathrm{Nu} = 2.45\left[\left(1 - \varepsilon\,\mathrm{KoLu}\frac{\mathrm{Ki}_m}{\mathrm{Ki}_q}\right)X\right]^{0.5};$$

$$\text{Stage II} \qquad (X > X_q^{ss})\ \mathrm{Nu}_{\min} = 6 = \text{const}.$$

In the initial section ($X < X^{ss}$) the temperature and potential distributions stabilize, and this stabilization of the temperature tends to reduce the heat-transfer rate. The length of the thermal-stabilization section increases in the presence of mass transport, while the heat-transfer rate increases with the values for the phase-transition, Lykov, and Kossovich criteria, i.e., with $\varepsilon\mathrm{KoLu}(\mathrm{Ki}_m/\mathrm{Ki}_q)$. The mass transfer has no effect in the region of stabilized heat transfer, and the values for $\mathrm{Nu}_{\min}$ are identical with and without mass transfer.

Dep. 387-79, Dec. 19, 1978.
Original article submitted June 20, 1978.

## FREE CONVECTION IN LAYERS OF POWDERED BUILDING MATERIALS

I. Ya. Neusikhin and V. V. Pokotilov

UDC 536.24

Measurements have been made on the heat-transfer rate in free convection for horizontal layers of actual building materials of comparatively large grain size (d = 5-40 mm); such a system cannot be taken as isotropic, but instead must be considered as consisting of a middle layer and two boundary layers, with the latter two layers more permeable and more porous than the middle layer.

The experiments were performed in the steady state. Radiative heat transfer in the bed was eliminated and the stability limit was attained for small temperature gradients by using deaerated water. The apparatus consisted of a conductance meter, power supplies, and various

*All-Union Institute of Scientific-Technical Information.

Translated from Inzhenerno-Fizicheskii Zhurnal, Vol. 36, No. 6, pp. 1108-1125, June, 1979.

0022-0841/79/3606-0731$07.50  

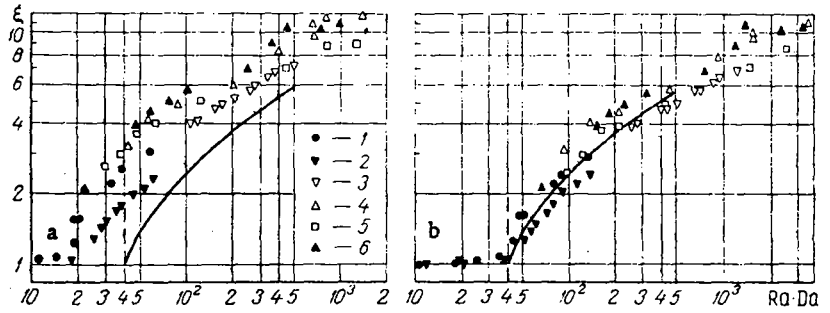


Fig. 1. Relationship between $\xi$ and Ra·Da; a) $\varkappa = \varkappa_c$; b) $\varkappa = \overline{\varkappa}$; solid line numerical solutions [8-10]; 1) H = 0.019 m and 2) H = 0.027 m for grit of 5-10 mm; 3) 0.046; and 4) 0.074 for grit of 10-20 mm; 5) 0.047; 6) 0.083 for grit of 20-40 mm.

measuring instruments. The conductance meter was of cylinder-piston type, which provided layers of various thicknesses. A flat electric heater provided the appropriate heat flux.

The measurements were made with layers of building grit of three size ranges: 5-10, 10-20, and 20-40 mm; values were determined for Ra·Da together with the corresponding $\xi$. The bed permeability $\varkappa$ appears in Da, and this in one case was taken as the permeability $\varkappa_m$ of the middle layer, while in the other it was taken as the bulk permeability $\overline{\varkappa}$ [1]. Graphs of $\xi = f$ (Ra·Da) (Fig. 1) were drawn up.

In the first case (a) the system was thus taken as isotropic, while in the second (b) it was taken as consisting of middle and boundary layers. Figure 1 shows that the results are of smaller spread in the second case and fit better to the theoretical relationship, which can be approximated by

$$\varepsilon = \lambda_{eq}/\lambda^* = 1 + 0.105\,[(\mathrm{Ra}\cdot\mathrm{Da}) - 40]^{0.64}.$$

These results indicate that such a bed should be considered as anisotropic at the boundaries, on account of the pressure gradient due to convection, especially in a system consisting of rough particles of random shape and comparatively large size.

LITERATURE CITED

1. I. Ya. Neusikhin and V. V. Pokotilov, Inzh.-Fiz. Zh., 34, No. 4 (1978).

Dep. 708-79, Jan. 18, 1979.
Original article submitted Apr. 21, 1978.

## QUASIREGULAR STATE IN HEAT AND MASS TRANSFER

V. M. Kazanskii

UDC 536.7:536.24

The paper deals with the general principles of quasiregular transfer of several substances; these principles, which have been formulated previously by the author, are here applied to heat transfer, alone or with mass transfer. Entropy calculation shows that the quasiregular state is the same as the regular state for pure heat transfer on a plate. Special features of the quasiregular state are considered for heat and mass transfer on a plate with boundary conditions of the third kind. The quasiregular principles (maximum entropy for constant mean values for the transport potentials) do not conflict with existing views on regular thermal and mass-transfer processes; instead, they constitute a generalization of the latter.

Dep. 714-79, Oct. 12, 1978.
Original article submitted Apr. 25, 1977.

# EFFECT OF LIFT ON HEAT TRANSFER AND FRICTION IN COMBINED CONVECTION

V. I. Dubovik

UDC 536.244:532.528

A slow flow around a permeable surface is considered, where the lift and the related free motion are opposite in direction to the forced flow.

A model is used for a vertical permeable (porous) surface parallel to the unperturbed flow.

Iterative fitting has been used in solving the boundary-layer equations, which have been transformed to ordinary differential equations subject to given laws for the distributions of the surface temperature and speed of the unperturbed flow. Dimensionless distributions have been derived for the velocity, temperature, and heat fluxes in the boundary layer for various values of the parameters representing the lift and the injection (suction) for a Prandtl number of 0.7. The results are presented as curves for $Nu/Nu_0$ and $f''(0)/f_0''(0)$ in relation to the injection (suction) for various values of the parameter that governs the effects of lift on the heat transfer and friction when the free and forced flows are opposite in direction.

The velocity distribution in the boundary layer indicates that the flow becomes detached when the parameter characterizing the lift becomes 0.95 of that for an impermeable surface.

Dep. 3750-78, Aug. 28, 1978.
Original article submitted Apr. 19, 1978.

# USE OF A CONSTANT-POWER FLAT HEATER IN DETERMINING THE THERMOPHYSICAL CHARACTERISTICS OF A TWO-LAYER MATERIAL

I. Ya. Neusikhin

UDC 536.2

A method is given for determining the thermophysical characteristics of an integral two-layer structure in terms of the temperature variation at a heater of constant output placed between two identical pieces of the material [1].

The observed $T(0, \tau) = f(\tau)$ relation can yield all the thermophysical characteristics of the layer closer to the heater (the boundary layer, denoted by subscript b) and the thermal-activity coefficient for the remoter main layer, which is denoted by subscript zero.

The following form applies [2] for the solution to the heat-conduction equation for constant boundary conditions of the second kind for the surfaces in contact with the heater:

$$T(0, \tau) = \frac{2q\sqrt{\tau}}{b_b}\left[\frac{1}{\sqrt{\pi}} + 2\sum_{1}^{\infty}(-h)^n \operatorname{ierfc}\frac{n}{\sqrt{Fo_b}}\right]. \quad (1)$$

Figure 1 shows (1) in $T(0, \tau)$ and $\sqrt{\tau}$ coordinates.

For $Fo_b < 0.2$, the temperature variation at the heater is governed only by the thermophysical characteristics of the boundary layer, as defined by (2), section o, e:

$$T(0, \tau) = \frac{2q\sqrt{\tau}}{b_b\sqrt{\pi}}. \quad (2)$$

The thermophysical characteristics of the main layer also begin to influence the heater temperature as $Fo_b$ increases, and the result is then dependent on the $K_b$. If $K_b = 1$, the heater temperature varies along line 1, which arises from the origin, while for $K_b = 0$ ($b_0 = \infty$) and for large $Fo_b$ we have that (1) becomes

$$T = T(0, \tau)|_{T(\delta_b, \tau)=T_0=\text{const}} = qR_b. \quad (3)$$

The line o, e gradually goes over to line 2. The line o, e also goes over gradually to a

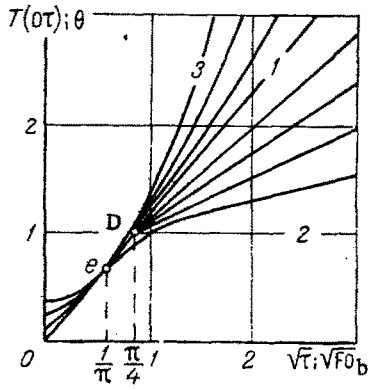


Fig. 1. Heater temperature variation in relation to thermal-activity coefficients of layers ($b_b$ and $b_o$).

straight line for intermediate values of $K_b$, and each of these lines is inclined to the $\sqrt{\tau}$ axis. The form of (1) is [3] as follows for $K_b = \infty$ ($b_o = 0$) and large values of $Fo_b$:

$$T(0, \tau) = qR_b(Fo_b + 1/3), \tag{4}$$

while the o, e line becomes the parabola 3. The o, e line goes over to a curve at point e for intermediate values of $K_b$.

It is also shown that, in $\theta$ and $\sqrt{Fo_b}$ coordinates, all the curves to the right of the line in position 1 intersect the o, e curve at point D, no matter what the thermophysical characteristics of the materials, and this point has coordinates $\theta = 1$, $Fo_b = \pi/4$, while all the curves to the left of line 1 are parabolas of variable degree (0.5 in position 1, 1 in position 3), and they are tangential to the o, e curve at point e, which has coordinates $\theta = 0.645$, $Fo_b = 1/\pi$.

These arguments allow one to use the temperature variation at the heater to solve the problem. Working formulas are given.

## NOTATION

$T(0, \tau)$, heater temperature; q, heat flux; $\tau$, time; $h = (1 - K_o)/(1 + K_b)$; $K_b = b_1/b_o$; $b = \sqrt{\lambda c\rho}$; $Fo_b = a_b\tau/\delta_b^2$; $a_b = \lambda_b/c_b\rho_b$; $\delta_b$, boundary-layer thickness; $R_b = \delta_b/\lambda_b$; $\theta = T(0, \tau/T)$.

## LITERATURE CITED

1. A. B. Verzhinskaya and L. N. Novichenok, "A new universal method of determining thermophysical constants," Inzh.-Fiz. Zh., No. 9 (1960).
2. I. Ya. Neusikhin and I. M. Chichkin, "An apparatus for examining conductive heat transfer for a powder in contact with a flat heater," Interdepartmental collection: Heating, Ventilation, and Building Thermophysics [in Russian], No. 3, Vyshéishaya Shkola, Minsk (1974).
3. A. I. Pekhovich and V. M. Zhidkikh, Calculations on Thermal Conditions in Solids [in Russian], Énergiya, Leningrad (1968).

Dep. 157-79, Nov. 23, 1978.
Original article submitted Nov. 2, 1977.

# INTERNAL DIFFUSION IN ELECTROMAGNETIC FIELDS

G. A. Vitkov, T. N. Zabelina, and T. M. Reier

UDC 532.546:532.72:538.4

Measurements are reported on the formation of solid films in droplets of viscose, and also the formation of viscose fibers in baths acted on by electric and magnetic fields. The

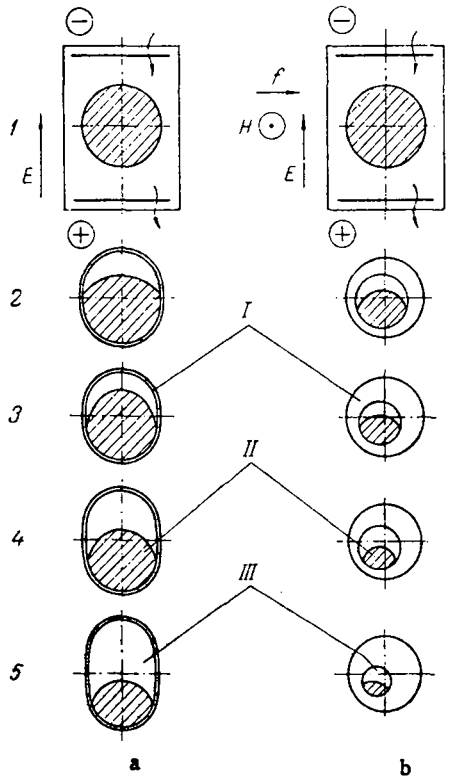


Fig. 1. Characteristic forms of droplet at various times t (sec): 1) 0; 2) 120; 3) 240; 4) 360; 5) 480; a) in an electric field of $E = 5.8 \cdot 10^2$ V/m at a precipitant concentration $C(H_2SO_4)$ = 75 g/liter; b) in an electromagnetic field having $E = 3.48 \cdot 10^2$ V/m, $H = 8 \cdot 10^5$ A/m, and the same concentration; I) cellulose hydrate layer; II) viscose; III) xanthogenate layer.

laboratory system consisted of a flat cell containing two electrodes, a temperature-control system, and an electrode power supply. Measurements were made on the boundaries of the reaction zones in the drop at various times after the start. Parts a and b of Fig. 1 show characteristic drop shapes at various times in an electric field (a) and in the presence of electromagnetic forces (b).

The results are as follows:

1. An electric field accelerates the precipitation of cellulose xanthogenate by ion transport in the viscose–bath system.

2. The processes in the magnetic field are generally as under ordinary conditions, but the rates are somewhat higher.

3. The precipitation of cellulose xanthogenate and the decomposition to cellulose hydrate are both accelerated in the presence of electromagnetic forces.

Measurements are reported on the acceleration of the formation of viscose fibers in electromagnetic fields, and it is shown that these fields can be used to accelerate the processes in the presence of reactions giving rise to capillary structures in cellulose hydrate fibers.

Dep. 154-79, Oct. 4, 1978.
Original article submitted July 25, 1977.

# OPERATING PRINCIPLES AND APPLICATIONS OF EQUIPMENT WITH GAS-CONDENSATION COOLING

F. M. Chernomurov

UDC 536.584

Means of efficient replacement of water by gas (e.g., air) for cooling surfaces are considered, particularly for use in areas where the freshwater supply is restricted or environmental contamination must be avoided.

It is shown that heat-pipe techniques are of considerable value here [1].

The principle has been implemented in equipment with gas-condensation cooling, in which there is an isothermal distribution of the heat flux over a large surface, which is subsequently cooled by a gas.

The gas-cooled surface (condenser bank) is (Fig. 1) either within a sealed hollow vessel (a or d) or outside the latter (b, c, e). The vapor and condensate travel either along a common channel (a) or along separate channels (in the other cases), in accordance with the configuration of the condenser and the sealed chamber, while the separate channels may be outside the sealed vessel (b and c). The cooling gas passes within the pipes in the condenser section (b, d, and e). In some cases, it is desirable for the pipes in the condenser to have forced motion for the vapor, with the cooling gas circulating in the space between the tubes (c). If the condensation surface is extensive and appropriately finned, comparatively high heat flux densities can be handled by natural convection, i.e., forced circulation of the cooling gas is not necessary.

A description is given of the laboratory system, of the methods used in the experiments, and of some results obtained during measurements on the variations in heat-flux density in the heating zone, along with the required flow of cooling gas (air).

Results are given on the use of water as the intermediate heat carrier for a horizontal

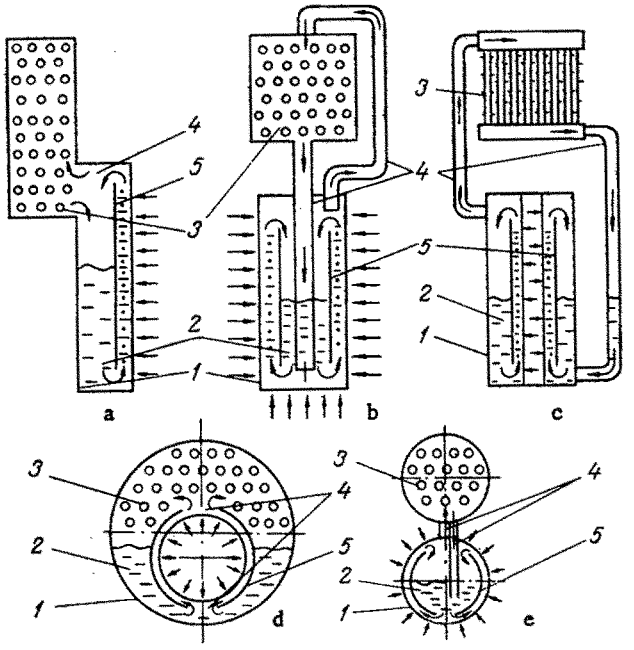


Fig. 1. Styles of equipment with gas-condensation cooling (arrows show heat supply zone and directions of movement of vapor and condensate); a, b, and c) cooling planes or cylindrical vertical surfaces; d, e) spherical or horizontal cylindrical cooling surfaces; 1) sealed body; 2) intermediate heat carrier; 3) condenser bank; 4) channel for vapor and condensate; 5) inserts.

planar cooled surface; the system has been found to be highly stable and reliable. Also, there is a very much reduced probability of contaminating the air with harmful pollutants, as well as a reduction in the demand for fresh water, while it is comparatively easy to utilize the waste heat.

It is concluded that this system should be widely used in industrial plants in arid areas or anywhere lacking plentiful fresh water.

## LITERATURE CITED

1. L. L. Vasil'ev and S. V. Konev, Heat-Transfer Pipes [in Russian], Nauka i Tekhnika, Minsk (1972).

Dep. 158-79, Oct. 16, 1978.
Original article submitted Apr. 6, 1978.

# CALCULATION OF THE WATER CONTENT OF SATURATED COMPRESSED AIR

V. M. Braun

UDC 533.275.001.24

The water content of air can be calculated from Dalton's law only if the pressure of the vapor–air mixture is comparatively low, in which case each component can be considered as an ideal gas.

No analytical formulas are available for the water content of air at high pressures, so computers cannot be employed, and in that case one normally uses a nomogram [1] constructed from the measurements of [2].

The water content of saturated compressed air is given by

$$d_s = 0.6221 \frac{P_s}{P - P_s} [1 + C(P - P_s)], \text{ kg/kg of dry air}. \quad (1)$$

The value of C may be calculated from the data of [2] or approximated by the polynomial

$$C = a_0 + a_1 \frac{T}{100} + a_2 \left(\frac{T}{100}\right)^2 + a_3 \left(\frac{T}{100}\right)^3. \quad (2)$$

The working range for the measurements is $-35°C \leqslant t \leqslant 50°C$, $P \leqslant 20$ MPa (200 kgf/cm$^2$).

The vapor pressure of water in the range ±90°C is

$$P_s = \exp\left(b_0 + \frac{b_1}{T} + b_2 \ln T + b_3 T + b_4 T^2\right) \text{MPa}. \quad (3)$$

Equations (1)-(3) fit the input experimental data with a mean deviation in water content of 2.1%.

## NOTATION

$d_S$, mass water content; P, total pressure of vapor–gas mixture; $P_S$, partial pressure of water vapor in saturated air; T, absolute temperature.

TABLE 1. Tabulated Coefficients of (2) and (3)

| $T$ | Coeff. | Subscript 0 | 1 | 2 | 3 | 4 |
|---|---|---|---|---|---|---|
| $T<273$°K | $a$ | 7,9237 | —8,2447 | 2,8951 | —0,34124 | — |
| | $b$ | —24,48667 | —5631,1202 | 8,2312 | —0,03861448 | $2{,}774937\times10^{-5}$ |
| $T>273$°K | $a$ | 2,5944 | —2,2516 | 0,65806 | —0,064071 | — |
| | $b$ | 63,53019 | —7235,4242 | —8,2 | 0,0057113 | 0 |

LITERATURE CITED

1. E. M. Landsbaum, W. S. Dodds, and L. F. Stutzman, Ind. Eng. Chem., 47, No. 1 (1955).
2. T. J. Webster, J. Soc. Chem. Ind., 69, No. 11 (1950).

Dep. 62-79, Nov. 22, 1978.
Original article submitted May, 24, 1977.

# COOLING OF A HEAT BRIDGE BY HELIUM VAPOR IN THE PRESENCE OF LOCALIZED HEAT SOURCES

B. V. Eliseev, Yu. P. Mordvinov, and I. V. Ufatov

UDC 621.396.6-181.48.017.7

The thin-fin approximation is used in determining the temperature distribution in each of two helium-cooled parts of a thermal bridge placed one behind the other, where heat is provided at the start of the second part. Differential equations are written for the temperature of the bridge material and of the helium on the basis of heat transfer by laminar or turbulent flow. The temperature of the helium is given along with the temperature of the bridge material (1Kh18N10T steel) at the start of the first part, as well as the temperature of the material at the end of the second part; the temperature is continuous at the junction between the parts, while the derivatives with respect to the coordinate differ by an amount $q/\lambda$. The equations have been solved by computer. The temperature distribution over the length of the bridge is determined along with the heat fluxes at the cold and warm ends for various helium flow rates and for various heat fluxes at the junction between the two parts, as well as for various geometrical parameters of the bridge.

Figure 1 shows the heat flux at the cold end of the bridge as a function of the additional heat flux at the junction; as the flux decreases (and cooling sets in), there is a limit to the value of q for which $\lambda_0 T'|_0 = 0$.

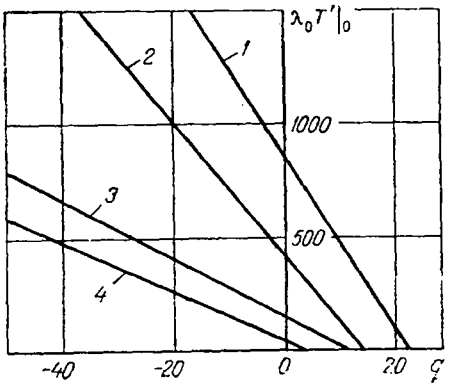


Fig. 1. Heat flux $\lambda_0 T'|_0$ at the cold end as a function of q for identical values of $S/\Pi l^2 = 1.11\ m^{-1}$ and various values of G: 1) G = 0.0001 kg/sec; 2) 0.0002; 3) 0.0005; 4) 0.001; $v_0$ = 0.1 m/sec; $T_0$ = 10°K; $T_{H_0}$ = 8°K; $T_e$ = 300°K.

## NOTATION

$\lambda(T)$, thermal conductivity of material, W/m·deg; G, helium flow rate, kg/sec; S, cross-sectional area of bridge, $m^2$; $\Pi$, perimeter of cross section, m; $l$, length of part of bridge, m; $v_0$, speed of helium at start of first part, m/sec; T, bridge temperature; $T_0$ and $T_{H_0}$, temperatures of bridge and helium at start of first part, °K; $T_e$, temperature at end of second part.

Dep. 160-79, Nov. 2, 1978.
Original article submitted Feb. 24, 1978.

## SCATTERING OF A MULTIMODE UHF FIELD IN A MOIST DIELECTRIC

Yu. K. Gubiev, A. G. Gasparyants, and V. V. Krasnikov

UDC 664.853.56

The dissipation of a multimode uhf field in a material is dependent on the structure of the field as well as on the physical parameters of the material; the electromagnetic field energy in a cavity resonator is the sum of the contributions from the modes. If the uhf waves are scattered and absorbed by liquids, including ones enclosed in colloidal or porous bodies, then the specific power $p_\nu$ absorbed from each mode is substantially dependent on the way in which the water is bound in the material. If we assume that the electric field strength is constant in a given microscopic volume, then the total specific power dissipation is

$$p_t = \sum_\nu p_\nu = 0.55 \cdot 10^{-10} f_g E_{ef}^2 \sum_\nu \varepsilon_\nu'' \ (\mathrm{W/m^3}), \tag{1}$$

where $\varepsilon_t'' = \sum_\nu \varepsilon_\nu''$ is the total loss factor at the generator frequency $f_g$ and $E_{ef}$ is the effective electric field vector.

It has been found [1] that dielectric losses at high input power levels (over 1 kW) should be determined by methods based on the actual energy absorption in the working frequency range, and an example of such a method is the calorimetric one.

The total specific power in the calorimetric load may be determined by neglecting phase-transition effects, and then (1) gives expressions for the effective electric field

$$E_{ef} = \sqrt{\frac{c_w \rho_w d\bar{t}}{0{,}55 \cdot 10^{-10} \varepsilon_{fr}'' f_g d\tau}} \tag{2}$$

and the total loss factor

$$\varepsilon_{t1}'' = \frac{\rho_0}{\rho_w} \left( \frac{c_0}{c_w} + \bar{U} \right) \varepsilon_{fr}'' \frac{d\bar{t}/d\tau}{d\bar{t}_1/d\tau}, \tag{3}$$

where $\rho_0$ and $c_0$ are the density and specific heat of the dry material; $\rho_w$ and $c_w$, density and specific heat of distilled water; $\bar{U}$, average water content of the material; $d\bar{t}/d\tau$, rate of change of the mean temperature of the moist insulator; and $d\bar{t}_1/d\tau$, rate of change in the mean temperature of distilled water in calorimetric measurement of the specific power.

Dep. 58-79, Nov. 9, 1978.
Original article submitted June 27, 1977.

## NUMERICAL INTEGRATION IN THE CALCULATION OF ANGULAR RADIATION COEFFICIENTS FOR A SYSTEM OF TWO PLANE-PARALLEL BODIES

A. V. Trofimenko and V. F. Prisnyakov

UDC 536.33

An algorithm and formula are given for calculating these coefficients by contour integration for two parallel rectangular bodies of areas $F_1$ and $F_2$. The rectangles are oriented in the planes with their sides mutually parallel (Fig. 1).

We give the following form [1] to the formula for the angular coefficient for plane-parallel surfaces:

$$\varphi_{1-2} = \frac{1}{2\pi F_1} \oint_{G_1} \oint_{G_2} (\ln S dx_2 dx_1 + \ln S dy_2 dy_1). \tag{1}$$

We integrate first over contour $G_2$ and then over $G_1$, which gives the coefficient as

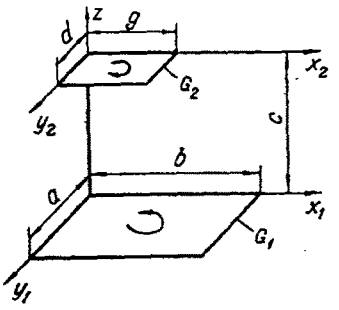


Fig. 1. Contour integration.

TABLE 1

| Trapezium formula | $h=k$ | $\varphi_{1-2}$ | $\Delta=\lvert\varphi_{1-2}-\varphi^*_{1-2}\rvert$ |
|---|---|---|---|
| | 1,0 | 0,83185 | 0,04412 |
| | 0,5 | 0,86476 | 0,01121 |
| | 0,25 | 0,87327 | 0,00270 |
| **Simpson's formula** | $h=k$ | $\varphi_{1-2}$ | $\Delta$ |
| | 1,0 | 0,85774 | 0,01823 |
| | 0,5 | 0,87573 | 0,00024 |
| | 0,25 | 0,87585 | 0,00012 |

$$\varphi_{1-2}=\frac{1}{2\pi F_1}\left[\int_0^a\int_0^d\ln\left[(x_2-x_1)^2+g^2+c^2\right]^{1/2}dx_2dx_1-\right.$$

$$-\int_0^a\int_0^d\ln\left[(x_2-x_1)^2+c^2\right]^{1/2}dx_2dx_1-\int_0^a\int_0^d\ln\left[(x_2-x_1)^2+(b-g)^2+c^2\right]^{1/2}dx_2dx_1+$$

$$+\int_0^a\int_0^d\ln\left[(x_2-x_1)^2+b^2+c^2\right]^{1/2}dx_2dx_1+\int_0^b\int_0^g\ln\left[(y_2-y_1)^2+a^2+c^2\right]^{1/2}dy_2dy_1$$

$$\left.-\int_0^b\int_0^g\ln\left[(y_2-y_1)^2+c^2\right]^{1/2}dy_2dy_1-\int_0^b\int_0^g\ln\left[(y_2-y_1)^2+(a-d)^2+c^2\right]^{1/2}dy_2dy_1+\int_0^b\int_0^g\ln\left[(y_2-y_1)^2+d^2+c^2\right]^{1/2}dy_2dy_1\right]. \quad (2)$$

The computation of the double integrals on the right in (2) has to be performed numerically; the trapezium formula or some other numerical method such as Simpson's formula is applied twice to derive standard relations for the integrals over a rectangular region.

The error in calculating these coefficients in this way has been determined by reference to a published formula [1,2]. The exact value has been calculated [2] for two parallel equal rectangles for A = a/c = 10, B = b/c = 20, and the result is accurate to the fifth significant figure and is $\varphi^*_{1-2}$ = 0.87597. Table 1 gives results from the trapezium formula and Simpson's rule when 10, 20, and 40 segments are used.

Clearly, numerical integration over the contour provides adequate accuracy in calculating the angular coefficients even when only a moderate number of segments is employed.

LITERATURE CITED

1. E. M. Sparrow and R. D. Cess, Radiation Heat Transfer, Brooks-Cole (1969).
2. A. G. Blokh, Principles of Radiative Heat Transfer [in Russian], Gosénergoizdat, Moscow–Leningrad (1962).

Dep. 63-79, Oct. 16, 1978.
Original article submitted Mar. 31, 1978.

# BEHAVIOR OF A GAS BUBBLE PASSING THROUGH A HORIZONTAL HOLE AT CONSTANT PRESSURE

V. V. Sobolev and P. M. Trefilov

UDC 532.529

There are several studies [1-4] on gas bubbles in liquids; two basic equations [4] are used in models describing gas bubbles formed in holes:

$$V(\rho-\rho')g=\left(\rho'+\frac{11}{16}\rho\right)(\dot{V}\dot{S}+V\ddot{S})+6\pi\mu\alpha\dot{S}, \tag{1}$$

$$P_1-\rho g(h-s)-\Delta P_\sigma-\frac{1}{k^2}(\dot{V})^2=\frac{\rho h\ddot{V}}{A}+\rho\left[\alpha\ddot{\alpha}+\frac{3}{2}\dot{\alpha}^2\right]+\frac{4\mu\dot{\alpha}}{\alpha}. \tag{2}$$

The quantity k is a coefficient in the formula that defines the relationship between the gas flow rate $\dot{V}$ and the total pressure difference across the hole [2,4], $\dot{V}=k(\Delta P)^{1/2}$; the second and fourth terms on the right in (2) describe, respectively, the hydrostatic loss and the pressure loss across the hole. The inertia of the liquid arising from the translational motion of the bubble and the inertia of the liquid surrounding the bubble arising from the radial fluctuations in the cavity are incorporated via the first and second terms, respectively, on the right in (2). The last terms on the right in (1) and (2) describe the effects of the viscous forces on the formation of the bubble.

An analytical discussion is presented for the behavior of $\alpha$ and S at small times; linear perturbation theory is used to show that there exists a critical radius $\alpha_*$ for $S<\alpha$ such that for $\alpha_0=\alpha(0)>\alpha_*=(\sigma/3\rho g)^{1/2}$ the bubble grows at the hole if the inertial effects are neglected, whereas for $\alpha<\alpha_*$ the bubble will pulsate with the natural frequency

$$\beta=\sqrt{\frac{8g}{11\alpha_0}\left(\frac{3\alpha_0^2\rho g}{\sigma}-1\right)}.$$

There is a certain increase in $\alpha_*$ on incorporating the inertia.

Numerical integration of (1) and (2) has been used to examine the behavior; the calculations were carried to the instant of detachment, at which $\alpha=S$. The behavior of cavities in water, liquid iron, and glycerol was examined. It was found that the detachment time decreases as the height of the liquid h increases, which is due to decrease in the radius of the bubble arising from increased hydrostatic pressure, with a corresponding reduction in the upthrust.

## LITERATURE CITED

1. S. S. Kutateladze and M. A. Styrikovich, Hydraulics of Gas–Liquid Systems [in Russian], Nauka, Moscow (1958).
2. J. F. Davidson and B. O. Schüler, Trans. Inst. Chem. Eng., 38, 144 (1960).
3. O. E. Potter, Chem. Eng. Sci., 24, 1734 (1969).
4. R. D. La Nauze and I. J. Harris, Chem. Eng. Sci., 27, 2102-2105 (1972).

Dep. 159-79, Nov. 9, 1978.
Original article submitted Mar. 28, 1978.

# GENERAL TEMPERATURE PATTERN IN A SPACE CONTAINING A DESCENDING CAVITY

M. P. Lenyuk and Z. L. Seredyuk

UDC 536.21

The dynamic temperature distribution is derived for a homogeneous isotropic space containing the cavity $D=\{(r,\theta,\varphi),\ 0\leqslant r\leqslant R,\ 0\leqslant\theta\leqslant\theta_0,\ 0\leqslant\varphi<2\pi\}$ on the assumption that the relaxation time $\tau_r$ for the thermal stresses is independent of direction; the distribution is described by a scalar quantity T that is the solution to a hyperbolic heat-conduction equation [1]:

$$b_0^2\frac{\partial^2 T}{\partial t^2}+b_1^2\frac{\partial T}{\partial t}-\left(\frac{\partial^2 T}{\partial r^2}+\frac{2}{r}\frac{\partial T}{\partial r}+\frac{1}{r^2}\left\{\frac{\partial}{\partial\mu}\left[(1-\mu^2)\frac{\partial T}{\partial\mu}\right]+\frac{1}{1-\mu^2}\frac{\partial^2 T}{\partial\varphi^2}\right\}\right)=f_1(t,\ r,\ \mu,\ \varphi),\ \mu=\cos\theta \tag{1}$$

subject to the initial and boundary conditions

$$T\Big|_{t=0}=f_2(r,\ \mu,\ \varphi),\ \frac{\partial T}{\partial t}\Big|_{t=0}=f_3(r,\ \mu,\ \varphi), \tag{2}$$

$$\left[-\frac{\partial}{\partial r}+\beta_1 h\left(1+\beta_2\tau_r\frac{\partial}{\partial t}\right)\right]T\Big|_{r=R}=h\psi(t,\ \mu,\ \varphi), \tag{3}$$

$$\lim_{r\to\infty}\left(\sqrt{r}\frac{\partial T}{\partial r}\right)=0,\ T\Big|_{\mu=\mu_0}=f_5(t,\ r,\ \varphi),\ \mu_0\leqslant\mu\leqslant 1,\ \mu_0=\cos\theta_0$$

and conditions representing uniqueness in $\varphi$; here $b_0^2=c_q^{-2}$; $b_1^2=a^{-1}$, and h is the relative heat-transfer coefficient, while $\beta_k$ (k = 1, 2) are the connectivity coefficients for the boundary conditions, and the function is

$$\psi(t,\ \mu,\ \varphi)=\left(1+\beta_2\tau_r\frac{\partial}{\partial t}\right)f_4(t,\ \mu,\ \varphi).$$

The solution to (1)-(3) is constructed by Laplace transformation with respect to the time variable t and Legendre–Fourier transformation with respect to $\varphi$ and $\mu$, the result being

$$T=\int_0^t\int_R^\infty\int_{\mu_0}^1\int_0^{2\pi}E(r,\ \rho,\ t-\tau,\ \mu,\ \eta,\ \varphi-\alpha)\,f_1(\rho,\ \tau,\ \eta,\ \alpha)\,\rho^2\,d\alpha d\eta d\rho d\tau+$$

$$+\int_R^\infty\int_{\mu_0}^1\int_0^{2\pi}E(r,\ \rho,\ t,\ \mu,\ \eta,\ \varphi-\alpha)\,[b_1^2 f_2(\rho,\ \eta,\ \alpha)+b_0^2 f_3(\rho,\ \eta,\ \alpha)]\,\rho^2 d\alpha d\eta d\rho+$$

$$+b_0^2\int_R^\infty\int_{\mu_0}^1\int_0^{2\pi}E(r,\ \rho,\ t,\ \mu,\ \eta,\ \varphi-\alpha)\,f_2(\rho,\ \eta,\ \alpha)\,\rho^2 d\alpha d\eta d\rho+$$

$$+\int_0^t\int_R^\infty\int_0^{2\pi}W_\theta(r,\ \rho,\ t-\tau,\ \mu,\ \varphi-\alpha)\,f_5(\rho,\ \tau,\ \alpha)\,d\alpha d\rho d\tau+\int_0^t\int_{\mu_0}^1\int_0^{2\pi}W_r(r,\ t-\tau,\ \mu,\eta,$$

$$\varphi-\alpha)\,\psi(\tau,\ \eta,\ \alpha)\,d\alpha d\eta d\tau, \tag{4}$$

where E, $W_\theta$, $W_r$ are the principal solutions to the corresponding boundary-value problems. The structure of the principal solutions is presented separately for small values of the time.

In particular, it is found that: a) if the functions $f_j$ ($j=\overline{1,\ 5}$) are independent of the angular coordinate $\alpha$, then the function $T_1(r,\ t,\ \mu)$ describes the temperature-field structure in a space containing a spherical–conical cavity, and b) the function $T_2=\lim\limits_{\mu_0\to -1}T$ describes the structure of the temperature pattern in a space containing a spherical cavity, and c) the function $T_{par}=\lim\limits_{b_0\to 0}T$ describes ordinary parabolic temperature patterns in that space, and d) the function $T_b=\lim\limits_{b_1\to 0}T$ describes the structure of a pure wave pattern in that space.

## LITERATURE CITED

1. A. V. Lykov, Theory of Thermal Conduction [in Russian], Vysshaya Shkola, Moscow (1967).

Dep. 161-79, Sept. 17, 1978.
Original article submitted Mar. 13, 1978.

# AN ASYMPTOTIC SOLUTION TO A NONSTATIONARY HEAT-CONDUCTION EQUATION WITH TEMPERATURE-DEPENDENT TRANSPORT COEFFICIENTS

Yu. A. Pshenichnov

UDC 536.2.001

The paper discusses the boundary-value problem

$$C(T)\frac{\partial T}{\partial \mathrm{Fo}} = \frac{\partial}{\partial x}\left[\lambda(T)\frac{\partial}{\partial x}\right], \tag{1}$$

$$T(0, \mathrm{Fo}) = T_s(\mathrm{Fo}),\ T(l, \mathrm{Fo}) = T_0,\ T(x, 0) = T_0, \tag{2}$$

where the specific heat C(T) and the thermal conductivity $\lambda(T)$ are any analytic functions of temperature T, $T_s(0) = T_0$.

The variables are replaced in accordance with the following formulas:

$$\xi = x/2\sqrt{\mathrm{Fo}},\ \eta = \sqrt{\mathrm{Fo}},\ \vartheta(\xi, \eta) = T(x, \mathrm{Fo})$$

to transform the equations for small times to

$$\frac{\partial}{\partial \xi}\left[\lambda(\vartheta)\frac{\partial \vartheta}{\partial \xi}\right] + 2\xi C(\vartheta)\frac{\partial \vartheta}{\partial \xi} = 2\eta C(\vartheta)\frac{\partial \vartheta}{\partial \eta}, \tag{3}$$

$$\vartheta(0, \eta) = T_s(\eta^2),\ \vartheta(\infty, \eta) = T_0,\ \vartheta|_{\eta=0} = T_0. \tag{4}$$

The right and left sides of (3) and of the boundary conditions (4) are expanded as Taylor series in powers of $\eta$ near $\eta = 0$ to get a sequence of linear boundary-value problems for which the following special functions are introduced: $\omega_{41}(\xi)$, $\omega_{42}(\xi)$, $\omega_{61}(\xi)$, $\omega_{62}(\xi)$, $\omega_{63}(\xi)$, $\omega_{67}(\xi)$ (Fig. 1). The asymptotic solution to the initial boundary-value problem of (1) and (2) can then be put as

$$T(x, \mathrm{Fo}) = T_0 + 4T_2 i_2(\xi)\,\mathrm{Fo} + [32T_4 i_4(\xi) + T_2^2(\lambda_1\omega_{41} - C_1\omega_{42})]\mathrm{Fo}^2 + \\ + [384T_6 i_6(\xi) + T_2T_3(\lambda_1\omega_{61} - C_1\omega_{61}) - T_2^3[\lambda_1^2\omega_{62} + \lambda_1C_1(\omega_{63} + \omega_{65}) - C_1^2\omega_{66} - \lambda_2\omega_{67} + C_2\omega_{68}]]\,\mathrm{Fo}^3 + \ldots, \tag{5}$$

where $i_n(\xi) \equiv i^n\,\mathrm{erfc}(\xi)$ are integrals of the error function erfc($\xi$) and

$$\lambda_n = \frac{1}{n!}\frac{d^n\lambda}{dT^n}\Big|_{T=T_0},\quad C_n = \frac{1}{n!}\frac{d^nC}{dT^n}\Big|_{T=T_0},\quad T_n = \frac{1}{n!}\frac{d^nT_s}{d\eta^n}\Big|_{\eta=0}\ (n = 1, 2, \ldots);$$

$$\omega_{64} = 128(i_2i_4 - 3i_6) + \omega_{61},\ \omega_{65} = 4\omega_{41}i_2 - \omega_{62},\ \omega_{66} = 4\omega_{42}i_2 + \omega_{63},$$

$$\omega_{68} = \frac{64}{3}(i_2^3 - 6i_6) + \omega_{67}.$$

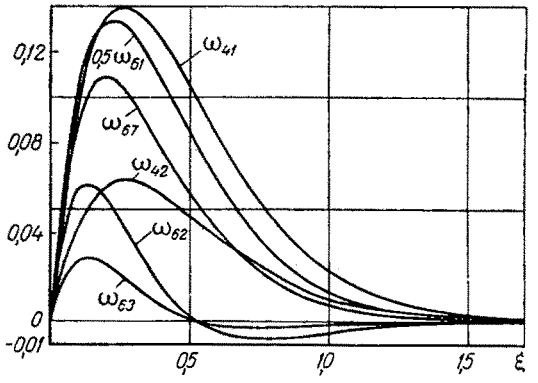


Fig. 1. Graphs of $\omega_{41}$, $\omega_{42}$, $0.5\cdot\omega_{61}$, $\omega_{62}$, $\omega_{63}$, $\omega_{67}$.

A comparison of calculations by this method and by finite-difference techniques indicates that the present method gives a useful formula for the temperature pattern at the initial stage of heating or cooling of an unbounded plate with variable thermophysical characteristics.

The asymptotic series of (5) can be used in constructing convenient algorithms for solving inverse problems in nonlinear heat conduction for small times.

Dep. 59-79, Aug. 22, 1978.
Original article submitted Jan. 10, 1978.

# THERMAL CONDUCTIVITY OF THE PERFORATED LEADING EDGE OF A GAS-TURBINE BLADE

E. N. Bogomolov

UDC 629.7.03:621.438:536.2

A one-dimensional approximation gives the temperature averaged over the wall thickness of the leading edge of a blade containing several rows of holes, for which purpose the equation of heat conduction has been solved for a bent unbounded plate:

$$\frac{d^2T_w}{dx^2} - \frac{\mathrm{Bi}_\Sigma}{\delta^2}(T_w - T_0) = 0,$$

and the solution of this for section j of the edge is written as

$$T_j - T_{0j} = A_j \exp\left(\frac{x}{\delta_j}\sqrt{\mathrm{Bi}_{\Sigma_j}}\right) + B_j \exp\left(-\frac{x}{\delta_j}\sqrt{\mathrm{Bi}_{\Sigma_j}}\right),$$

where

$$\mathrm{Bi}_\Sigma = \mathrm{Bi}_h\left[1 + \frac{\alpha_c}{\alpha_h}\left(1 - \frac{\delta}{R_h}\right)\right];\quad \mathrm{Bi}_h = \frac{\alpha_h\delta}{\lambda_w};\quad T_0 = \left[\alpha_h T_h + \alpha_c\left(1 - \frac{\delta}{R_h}\right)T_c\right]\Big/\left[\alpha_h + \alpha_c\left(1 - \frac{\delta}{R_h}\right)\right];$$

where T is temperature; x, a coordinate reckoned along the profile on the outer surface; $\delta$, wall thickness; R, radius of curvature; $\alpha$, heat-transfer coefficient; and $\lambda$, thermal conductivity, while the subscripts are w, wall; h, hot medium (gas); and c, cooling air.

The constants A and B are determined from the conditions at the boundaries; if it is assumed that there is a hole only at the start of each section, then we have

$$A_j = [a_{2j-1}(1 + S_j + C_{j-1,j})A_{j-1} + b_{2j-1}(1 + S_j - C_{j-1,j})B_{j-1} + S_j(T_{0j} - T_{a.sj}) + (1 + S_j)(T_{0j-1} - T_{0j})]/2a_{1j},$$

$$B_j = [a_{2j-1}(1 - S_j - C_{j-1,j})A_{j-1} + b_{2j-1}(1 - S_j + C_{j-1,j})B_{j-1} + S_j(T_{0j} - T_{a.sj}) + (1 - S_j)(T_{0j-1} - T_{0j})]/2b_{1j},$$

where

$$S_j = \frac{\mathrm{Bi}_{sj}}{\sqrt{\mathrm{Bi}_{\Sigma_j}}}\frac{\Phi_{sj}}{\delta_j H_j};\quad \mathrm{Bi}_{sj} = \alpha_{sj}\delta_j/\lambda_{cj};\quad C_{j-1,j} = \frac{\lambda_{cj-1}}{\lambda_{cj}}\sqrt{\frac{\mathrm{Bi}_{\Sigma_{j-1}}}{\mathrm{Bi}_{\Sigma_j}}};$$

$$a_{1j} = \exp\left(\frac{x_{1j}}{\delta_j}\sqrt{\mathrm{Bi}_{\Sigma_j}}\right);\quad a_{2j} = \exp\left(\frac{x_{2j}}{\delta_j}\sqrt{\mathrm{Bi}_{\Sigma_j}}\right);\quad b_{1j} = \exp\left(-\frac{x_{1j}}{\delta_j}\sqrt{\mathrm{Bi}_{\Sigma_j}}\right);$$

$$b_{2j} = \exp\left(-\frac{x_{2j}}{\delta_j}\sqrt{\mathrm{Bi}_{\Sigma_j}}\right),\quad \Phi_{sj}$$

is the internal surface of the perforations over a segment H along the length of the blade, and $T_{as}$ is the temperature of the air in the perforations.

The results for the central part of a symmetrical leading edge with 4 rows of perforations are

$$A = B = -\frac{2(T_0 - T_0') + [(2s + a_\Delta(1 + s_\Delta + c)s - b_\Delta(1 + s_\Delta - c)s](T_0 - T_{a*})}{a_\Delta(1 + s_\Delta + c)[a(2 + s) + bs] + b_\Delta(1 + s_\Delta - c)[-as + b(2 - s)]},$$

where

$$a = \exp\left(\frac{x_s}{\delta}\sqrt{\mathrm{Bi}_\Sigma}\right);\ b = \exp\left(-\frac{x_s}{\delta}\sqrt{\mathrm{Bi}_\Sigma}\right);\ a_\Delta = \exp\left(\frac{\Delta_s}{\delta}\sqrt{\mathrm{Bi}_\Sigma}\right);$$

$$b_\Delta = \exp\left(-\frac{\Delta_s}{\delta}\sqrt{\mathrm{Bi}_\Sigma}\right);\ C = \sqrt{\mathrm{Bi}_{i\Sigma}/\mathrm{Bi}'_\Sigma};$$

where s is the value of $S_j$ for the row of perforations at a distance $x_s$ from the center of the edge, $s_\Delta$ is the value of $S_j$ for the row of perforations at a distance $x_s + \Delta_s$ from the center of the edge, $\mathrm{Bi}'_\Sigma$, $T'_0$ correspond to the boundary parts of the edge (free from perforations), and $\mathrm{Bi}_\Sigma$, $T_0$ correspond to the inner parts of the edge (with perforations).

Calculations from these formulas agree satisfactorily with numerical determination of the temperature of isolated points made by Monte Carlo methods for boundary conditions of the third kind.

Dep. 3751-78, Aug. 14, 1978.
Original article submitted Dec. 20, 1977.

## SOME PROBLEMS IN THERMAL CONDUCTION FOR A WEDGE

O. B. Fedoseev

UDC 517.946:949

Many engineering processes involve temperature determination on wedges. A Mellin transformation applied to the Laplace operator in polar coordinates $\Delta T = 0$ can be used with the solution of the resulting differential equation to find the transform of the temperature in the form $\overline{T} = A \sin p\varphi + B \cos p\varphi$; the constants A and B are derived from the conditions at the faces of the wedge, while the integral in the formula for the inverse transformation is derived from the theory of residues and summation of the resulting series, which gives solutions in certain cases in terms of elementary functions. The symbol $\nu = \pi/(2\alpha)$ is used, where $\alpha$ is the angle of the wedge.

1. If zero temperature is maintained at the face $\varphi = 0$ of the wedge, while $\varphi = \alpha$ at the point $r = a$ corresponds to a localized heat flux Q on the thermally insulated face, then

$$T(r, \varphi) = \frac{Q}{2\pi\lambda} \ln \frac{1 + 2\rho \sin \nu\varphi + \rho^2}{1 - 2\rho \sin \nu\varphi + \rho^2},$$

where $\rho = (r/a)^\nu$ for $r \leq a$; $\rho = (a/r)^\nu$ for $r > a$ and $\lambda$ is the thermal conductivity.

2. If the face $\varphi = 0$ is thermally insulated, while $T = T_0$ for $r \leq a$ on the face $\varphi = \alpha$, and $T = 0$ for $r > a$, then we have

$$T(r, \varphi) = T_0 - \frac{T_0}{\pi} \operatorname{arctg} \frac{2(r/a)^\nu \cos \nu\varphi}{1 - (r/a)^{2\nu}} \text{ for } r \leq a;$$

$$T(r, \varphi) = \frac{T_0}{\pi} \operatorname{arctg} \frac{2(a/r)^\nu \cos \nu\varphi}{1 - (a/r)^{2\nu}} \text{ for } r > a.$$

3. If $T = 0$ on the face $\varphi = 0$, while $T = T_0$ for $r \leq a$ on the face $\varphi = \alpha$, and $T = 0$ for $r > a$,

$$T(r, \varphi) = \frac{\varphi}{\alpha} T_0 - \frac{T_0}{\pi} \operatorname{arctg} \frac{\sin 2\nu\varphi}{(a/r)^{2\nu} + \cos 2\nu\varphi} \text{ for } r \leq a;$$

$$T(r, \varphi) = \frac{T_0}{\pi} \operatorname{arctg} \frac{\sin 2\nu\varphi}{(r/a)^{2\nu} + \cos 2\nu\varphi} \text{ for } r > a.$$

A piecewise-constant flux on one of the faces has also been considered.

These solutions can be used in isolation or combined in engineering calculations.

Dep. 60-79, Oct. 16, 1978.
Original article submitted June 22, 1977.

# SOLUTION OF A DEGENERATE SINGLE-PHASE STEFAN'S PROBLEM FOR BOUNDARY CONDITIONS OF THE FIRST KIND AT THE BOUNDARY OF A HALF PLANE

A. M. Tsybin

UDC 536.2.01

Let $\varphi(\tau)$ be the temperature of the medium, which satisfies the conditions

$$-M < \varphi(\tau) < 0, \text{ where } M = \text{const} > 0, \tag{1}$$

$$\left| \int_0^{+\infty} \varphi(\tau) \exp(-p\tau)\, d\tau \right| < \frac{M}{|p|}, \quad \operatorname{Re} p > 0, \tag{2}$$

in which case the path followed by the zero isotherm $\xi(\tau)$ can be defined by solving a nonlinear integral equation derived by Grinberg and Chekmareva. It is assumed that $\varphi(\tau)$ satisfies (1) and (2) and can be represented as a power series

$$\varphi(\tau) = \sum_{r=0}^{\infty} \gamma_r \tau^r, \quad \gamma_0 < 0. \tag{3}$$

The unknown function $\xi(z)$ is expanded as

$$\xi^{2n}(z) = 2n \sum_{m=0}^{\infty} a_m^{(n)} \frac{z^{m+1}}{m+1} \quad (n = 1, 2, \ldots), \quad 0 \leqslant z \leqslant \tau, \tag{4}$$

to derive recurrence relations for the coefficients $a^{(n)}_m$, where $a$ is the thermal diffusivity and B is the result from dividing the enthalpy of the phase transition by the thermal conductivity of the material in the frozen zone:

$$a_1^{(1)}\left[1 + \sum_{i=2}^{\infty} \frac{2^{i-2}(a_0^{(1)})^{i-1}(i+1)!}{a^{i-1}(2i-1)!}\right] = -\frac{\gamma_1}{B}, \tag{5}$$

$$a_{k+1}^{(k+1)} = 2^{k-1}(a_0^{(1)})^k (k+2)\, a_1^{(1)} \quad (k = 1, 2, \ldots), \tag{6}$$

$$a_r^{(1)}\left[r! + \frac{1}{r+1} \sum_{i=r+1}^{\infty} \frac{2^{i-r}(a_0^{(1)})^{i-r}(i+1)!}{a^{i-r}[2(i-r)+1]!}\right] +$$

$$+\left\{\frac{(r+1)!}{3a}\sum_{n=1}^{r-1} a_n^{(1)} \frac{a_{r-n}^{(1)}}{r-n+1} + \sum_{i=r+2}^{\infty} \frac{i!}{a^{i-r}[2(i-r)+1]!} \sum_{j=1}^{i-r} 2^j (a_0^{(1)})^{j-1}\right.$$

$$\left. \times \sum_{n=i-r-j+1}^{i-j-1} a_n^{(i-r-j+1)} \frac{a_{i-n-j}^{(1)}}{i-j+1-n}\right\} = -\frac{\gamma_r}{B} r! \quad (r = 2, 3, \ldots), \tag{7}$$

$$a_{r+1}^{(2)} = a_0^{(1)} a_r^{(1)} (r+2) + 2\sum_{i=1}^{r-1} a_i^{(1)} \frac{a_{r-i}^{(1)}}{1+r-i} \quad (r = 2, 3, \ldots), \tag{8}$$

$$a_{k+r}^{(k+1)} = \frac{2^k (a_0^{(1)})^k}{r+1}(k+r+1)\, a_r^{(1)} + 2\sum_{i=k}^{r+k-2} a_i^{(k)} \frac{a_{r+k-i-1}^{(1)}}{r+k-i} +$$

$$+ \sum_{j=2}^{k} 2^j (a_0^{(1)})^{j-1} \sum_{i=k-j+1}^{r+k-j-1} a_i^{(k-j+1)} \frac{a_{r+k-i-j}^{(1)}}{r+k+1-i-j} \quad \begin{pmatrix} r = 2, 3, \ldots \\ k = 2, 3, \ldots \end{pmatrix}. \tag{9}$$

Examples are considered of the paths of the zero isotherm for the cases $\varphi(\tau) = -10 \exp(-\tau)$, °C; $\varphi(\tau) = -10[1 - \exp(-\tau)]$, °C; tables and graphs are presented. The temperature pattern in the frozen zone is then determined.

Dep. 61-79, Oct. 24, 1978.
Original article submitted June 3, 1977.

# HEAT TRANSFER AT A RAPIDLY MOVING BOUNDED CONTACT

A. P. Klenov, V. M. Makharinskii,
and V. F. Volkodavov

UDC 536.241:531.44

Nonstationary heat transfer is considered for bodies whose rectangular ideal contact generates heat of friction; rapid motion at a constant speed is envizaged. Various assumptions are made to reduce the three-dimensional treatment to a one-dimensional model. Laplace and Fourier integral transforms in a generalized-function space are employed. Approximate formulas are derived for the contact temperature or the heat fluxes in terms of the values averaged over the contact area; a comparison is made with analog simulation data and existing particular analytical solutions due to Jager and Lykov.

The problems considered here are related to many technical applications; the expressions for the contact temperature and heat fluxes are extremely general for large values of the Peclet number and serve to define solutions to many heat-transfer problems for bodies with contacts of rectangular form.

Dep. 155-79, Nov. 2, 1978.
Original article submitted Oct. 5, 1977.